

Structural Analysis of an Active Morphing Wing for Enhancing UAV Performance

E. Kaygan, A. Gatto

Abstract—A numerical study of a design concept for actively controlling wing twist is described in this paper. The concept consists of morphing elements which were designed to provide a rigid and seamless skin while maintaining structural rigidity. The wing structure is first modeled in CATIA V5 then imported into ANSYS for structural analysis. Athena Vortex Lattice method (AVL) is used to estimate aerodynamic response as well as aerodynamic loads of morphing wings, afterwards a structural optimization performed via ANSYS Static. Overall, the results presented in this paper show that the concept provides efficient wing twist while preserving an aerodynamically smooth and compliant surface. Sufficient structural rigidity in bending is also obtained. This concept is suggested as a possible alternative for morphing skin applications.

Keywords—Aircraft, morphing, skin, twist.

I. INTRODUCTION

MORPHING technologies typically revolve around adaptive geometries, structures, and mechanisms and remain attractive to aircraft designers. They possess the ability to provide substantial performance benefits to aircraft. The concept or ‘morphing’ however is not new. Wing warping mechanism were applied in 1903 by ‘The Wright Brothers’, to control – via wing twist using subtended cables [1] – the first powered, heavier than air, aircraft. The Wright Brothers intuitively considered aerodynamics, control, and structural aspects to achieve this revolutionary concept. However in today’s aviation world, while this particular technique is no longer suitable, the concept of ‘morphing’ to achieve greater efficiency remains very much relevant.

Ailerons, elevators, and rudder are the primary means for the control of aircraft today [2]. Although these all provide sufficient control performance, they can reduce aerodynamic efficiency due to strong surface curvatures that promote flow separation. To have more efficient aircraft, an argument exists for the re-examination of these traditional control surface methodologies, in favor of more “morphing-based” technologies and techniques [3]-[7]. Even with the possibility of substantial benefits, many limitations exist. Jha et al. [3] summarizes many of these technical challenges with the most significant structural design. This is particularly the case for a ‘morphing’ skin, which needs to maintain compliance (i.e. be flexible to actuate), but also sufficiently rigid to maintain and transfer aerodynamic loads to the internal structure. Previous

work on morphing skins has involved using FMC [8], [9], elastomeric [10], and/or corrugated skins [11], [12]; however, these, as yet, have not achieved widespread use. The problem remains achieving a skin with sufficient compliance and structural rigidity, while maintaining aerodynamic integrity.

In this paper, work is presented that details the structural design of a morphing roll control concept considered in an earlier paper [7]. The goal of this paper is to explore, specifically, structural design aspects of the twist concept using ANSYS environment. The work evaluates the rival requirements of resistance to wing bending, adequate twist compliance, and surface rigidity and continuity during twist actuation. To this end, the sections of this paper will describe the computational methodologies used, the integration of aerodynamic and structural loading, as well as evaluate the final design.

II. THE PROPOSED CONCEPT

The concept is shown in Fig. 1. The fundamental idea is to construct a wing (or portion thereof) using multiple, small thickness, rib sections assembled with span-wise stiffening elements (carbon rods), that are free to rotate and slide relative to one another. As a known limitation for previous morphing concepts, surface deformation and resistance to aerodynamic loading are controlled using the rigid, but finite nature of each rib element. Stiffening elements are needed (indicated in Fig. 1) to provide stiffness to the structure as well as maintain assembly cohesion. A main carbon tube is used at the quarter chord position to provide actuator torque. This element also provides structural stiffness and the facility for rib alignment. Finally, an end-section, mounted at the wing-tip, and fastened to the torque tube, transfers actuation torque to the rib elements (The schematic model chosen for this twist demonstration study is also shown in Fig. 1 (b)).

III. COMPUTATIONAL METHODOLOGY

A. Aerodynamic Load Prediction

AVL Method was used to estimate the aerodynamic response of a morphing wing. AVL is a simulation package that determines the solutions to a linear aerodynamic flow model. For all simulations, modelling was performed from a set of wing panels along the wing span and chord axes (computational

E. Kaygan is with the School of Aviation, Girne American University, Kyrenia, TRNC (e-mail: erdogankaygan@gau.edu.tr).

A. Gatto is with the College of Engineering, Design and Physical Sciences, Brunel University, Uxbridge, UB8 3PH, UK (e-mail: Alvin.Gatto@brunel.ac.uk).

model of wing structure is shown in Fig. 2). Using the “Biot-Savart law”, for each surface panel, an equation can be set up which is linear combination of the effects of the strengths of all panels. A solution for the strength of the vortex lines on each panel is found by solving matrix of equation. Aerodynamic forces and moments were then obtained from the solved load distribution by applying the “Kutta-Joukowski Theorem” [13].

For all simulations, the free-stream velocity was set to 30 m/s and all results were computed without the influence of compressibility. In order to be computationally efficient as well as to reduce computational time, a grid refinement study was completed on the baseline configuration prior to widespread use of the developed model.

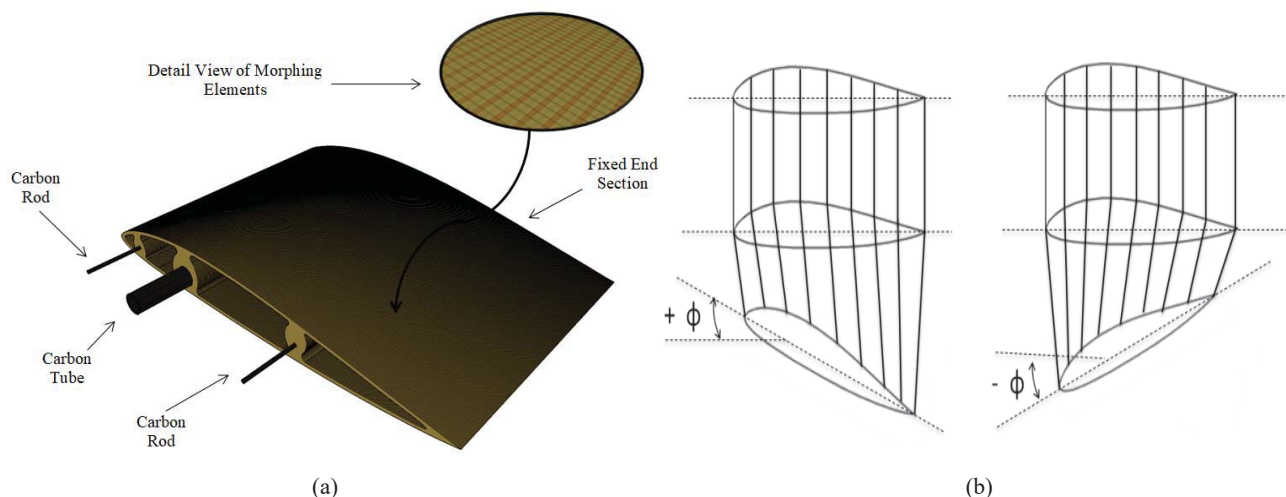


Fig. 1 Schematic view of an active wing: (a) Wing twist mechanism, (b) Positive twist angle (washin) and negative twist angle (washout)

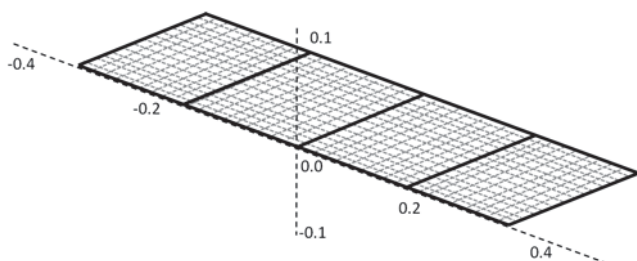


Fig. 2 Schematic of AVL models for active wing structure

B. Finite Element Model

The Finite Element Modelling (FEM) was carried out using ANSYS. The CAD design of the morphing wing and/or wingtip was achieved using CATIA V5 and then imported into ANSYS to evaluate the design structurally with aerodynamic loads extracted from AVL. Material properties supplied from individual experimental tests were thereafter applied (summarised in Table I). Overall, laser ply are used primarily for the ribs and carbon fibre for stiffening rods. To enact rib twist, the torque applied to the main carbon tube was transferred, via the end-section and stiffening rods, to the ribs. Overall, estimates of surface deformation, structural stresses, and wing tip deflection magnitudes were used as the primary parameters to evaluate structural performance.

TABLE I
SUMMARY OF MATERIAL PROPERTIES

Materials	Tensile Strength, MPa
Laser Plywood Sheets	70.93
P400 ABS Plastic	56.58
Carbon Fibre	600.00

Fig. 3 presents the boundary conditions applied to evaluate each model. For each rib, sliding contact (no separation) properties were used to achieve twist movements. Under these conditions, separation between ribs is not allowed (friction effects ignored), but frictionless sliding can occur. Each rib was connected to the stiffening rods via a sliding contact allowing free rotation during deformation. All three carbon rods were connected to the actuating end section with bonded constraints, which provided rotation of the end part and consequent rib twist. Totally, 4731 connections were used. To actuate the structure, a maximum 3.43 Nm of torque (based on the servomechanism used) were applied to the carbon tube.

Aerodynamic loading and pitching moments were also applied to each rib from segmented data reduced from AVL. Due to the need for accurate stress and deformation analysis, fine structural meshes were used. Body size meshing options were applied for only the small carbon rods (applied mesh to a wing model is shown in Fig. 4). This gives more accurate results for small surfaces and prevents over-meshing, which requires more computational power. A convergence study using a section of the wing was also performed to assess the suitability of the finite element mesh. Various meshing sizes were examined via changing the total element numbers from 350000 to 1600000 in steps of 50000 until the results exhibited insensitivity with further modification. Due to the computational memory and time requirements, 950000 elements were chosen as the final mesh size.



Fig. 3 Boundary conditions applied to morphing structures

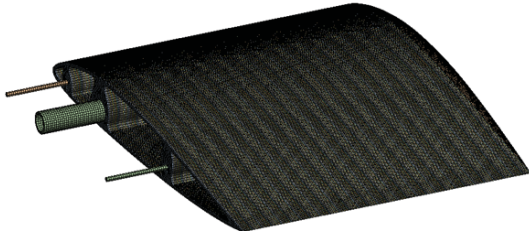


Fig. 4 Applied mesh to a wing model

IV. RESULTS AND DISCUSSION

For the morphing concept, optimising weight with an aerodynamically smooth surface finish were the main priorities. Assessments also needed to be made about overall strength as well the mechanism suitability. To assist in achieving these goals, several structural configurations were attempted. It is highly desirable to optimise rib structure with low wrinkling rate in order to achieve minimal drag. In this regard, maximum deformation criteria for a skin were defined based on boundary layer theory for a wing structure [14]. Accordingly, surface would move within a limit in the direction perpendicular to its normal vector to give the similar flow rate as ensues between the surface and the reference plane in an actual fluid [14]. A maximum displacement was calculated and based on these criteria, optimisation required for rib structures were

completed.

Five different rib edge thicknesses (t) were analysed (from $t=1\text{mm}$ to $t=3\text{mm}$ in steps of 0.5mm) to optimize the rib structure (parameter t is shown in Fig. 5). The results obtained from the FE static analysis were used to check compliance with structural requirements. The strength of each component is evaluated by comparing the Von Mises (VM) stress with the material yield strength. Table II summarizes the stresses on the carbon stiffening rods. It can be clearly seen that reducing rib edge thicknesses (t) increases stress on the carbon stiffening rods (in general, the maximum $\sigma = 463.14\text{ MPa}$ for $t=1\text{mm}$ was obtained on the rear carbon rod, well within the yield stress of 600 MPa). This would be expected as decreased rib edge thickness allows more twist (reducing weight also), but leads to greater forces applied to the carbon rods. Fig. 6 shows the results for $t=2\text{mm}$. These results show the highest stress occurs at the root of the wing structure (Fig. 6 (a)).

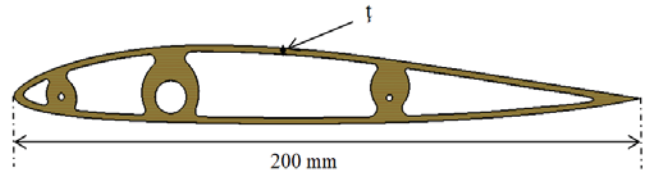
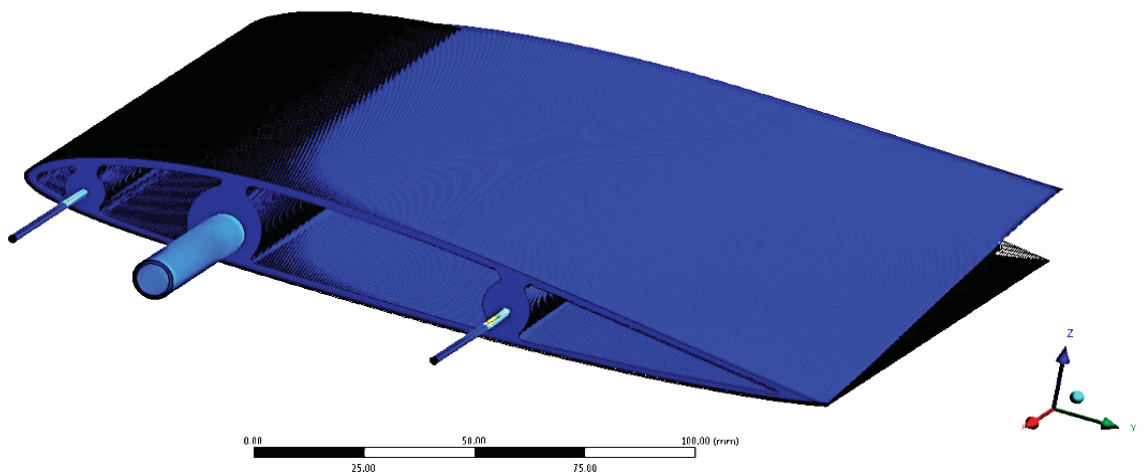
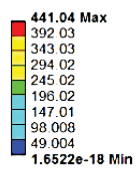


Fig. 5 Airfoil shape for an active wing concept

TABLE II
 SUMMARY OF STRESS ON CARBON RODS FOR VARIOUS RIB DESIGNS

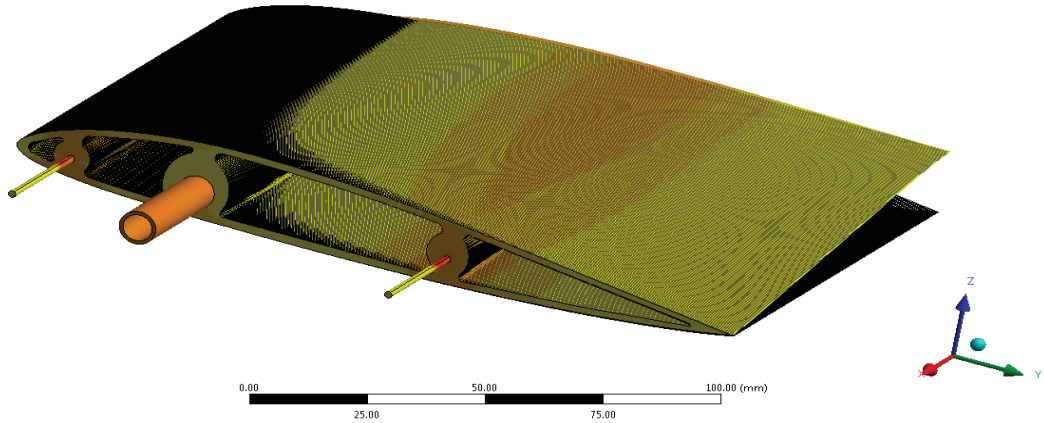
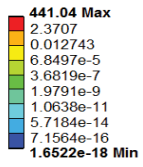
Rib Edge Thickness, t , mm	Wash-out σ_{max} , MPa	Wash-in σ_{max} , MPa
1	463.14	350.47
1.5	454.19	340.75
2	441.04	324.42
2.5	417.14	307.35
3	339.85	290.19

Static Structural
 Type: Equivalent (Von-Mises) Stress
 Unit: MPa



(a)

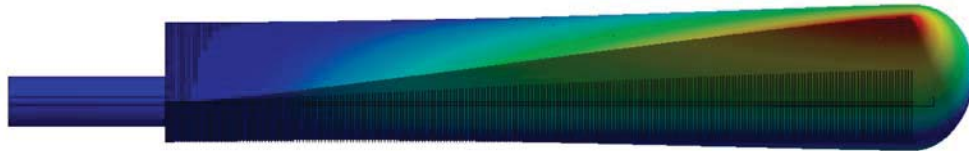
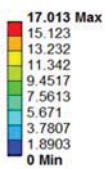
Static Structural
 Type: Equivalent (Von-Mises) Stress
 Unit: MPa



(b)

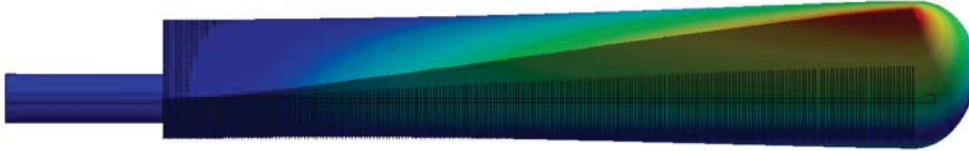
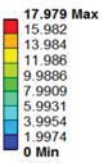
Fig. 6 Von-Mises Stress for $t=2\text{mm}$: (a) Von-Mises stress analysis and (b) Detail surface analysis of morphing concept

Static Structural
 Type: Total Deformation
 Unit: mm



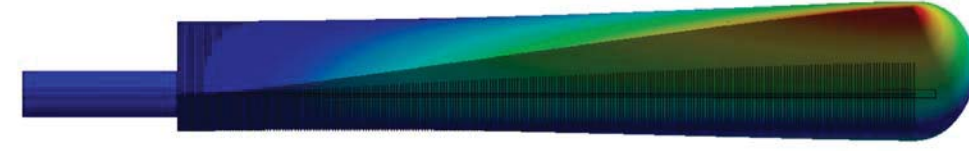
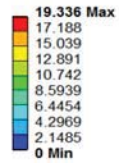
(a)

Static Structural
 Type: Total Deformation
 Unit: mm



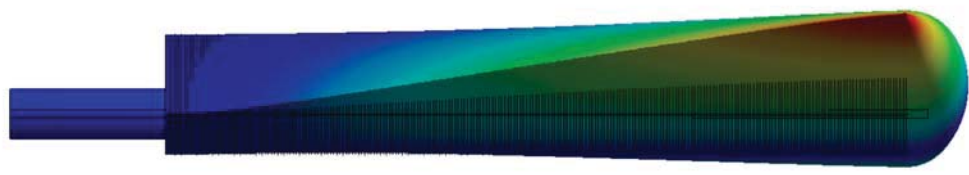
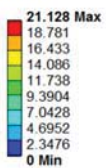
(b)

Static Structural
 Type: Total Deformation
 Unit: mm

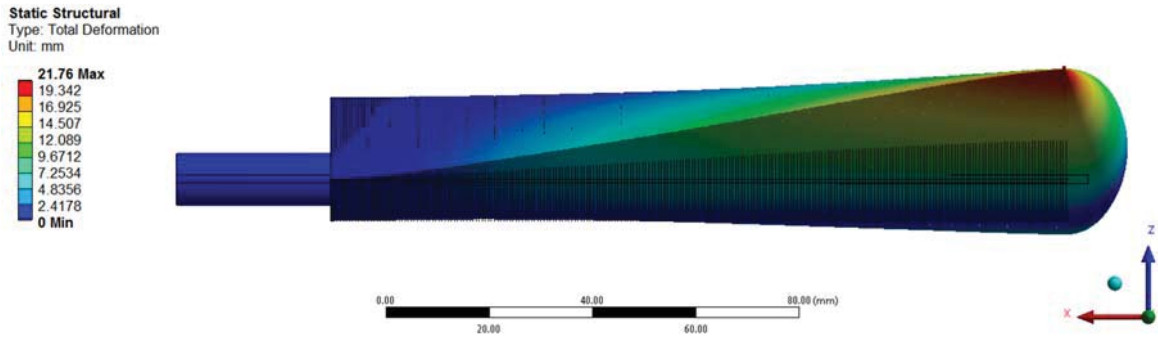


(c)

Static Structural
 Type: Total Deformation
 Unit: mm

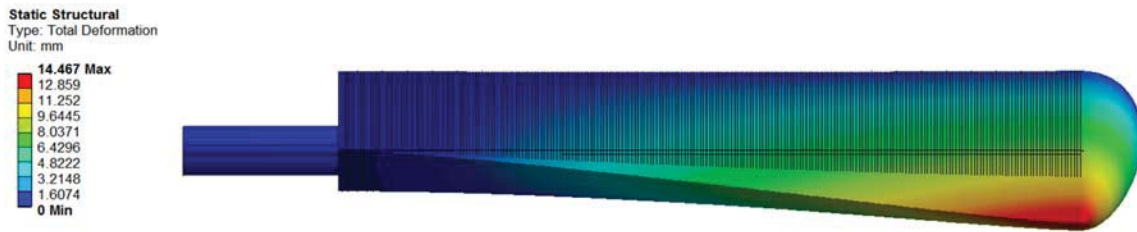


(d)

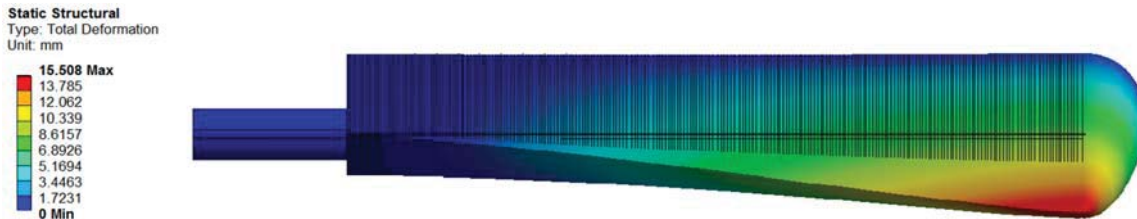


(e)

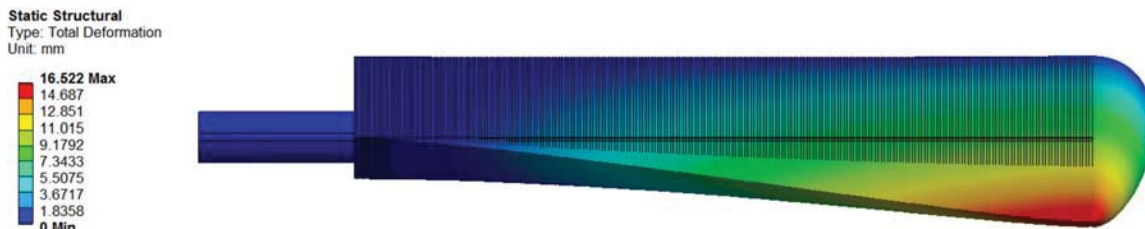
Fig. 7 Total twist deformation on morphing concept (Wash-out): (a) $\zeta=3\text{mm}$, (b) $\zeta=2.5\text{mm}$, (c) $\zeta=2\text{mm}$, (d) $\zeta=1.5\text{mm}$, and (e) $\zeta=1\text{mm}$



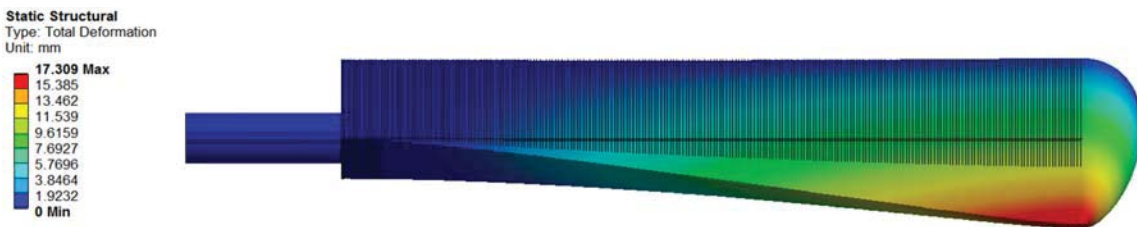
(a)



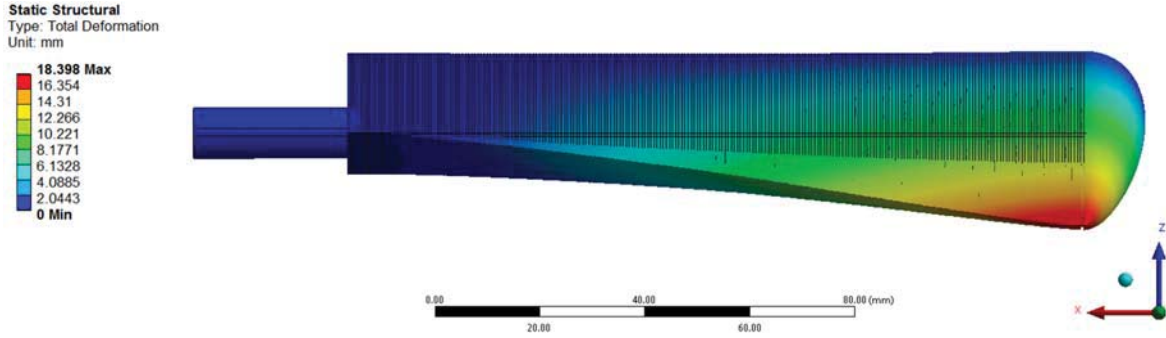
(b)



(c)

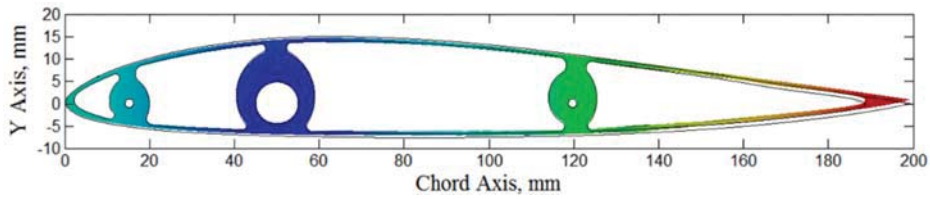


(d)

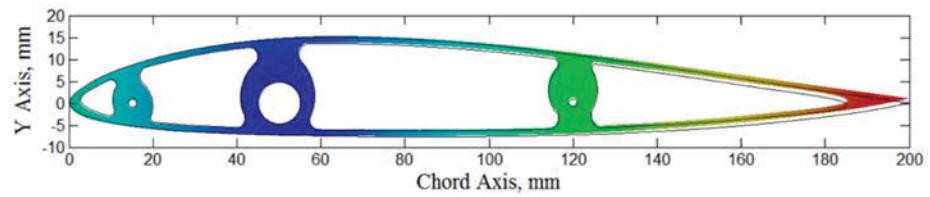


(e)

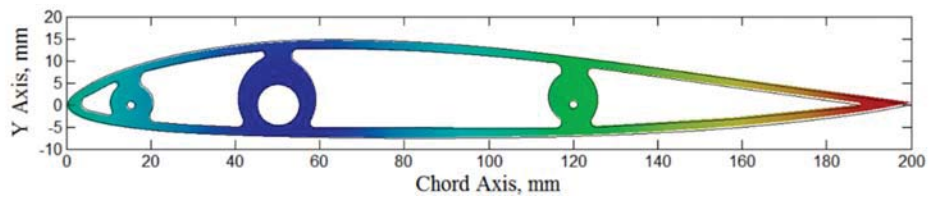
Fig. 8 Total twist deformation on morphing concept (Wash-in): (a) $t=3\text{mm}$, (b) $t=2.5\text{mm}$, (c) $t=2\text{mm}$, (d) $t=1.5\text{mm}$, and (e) $t=1\text{mm}$



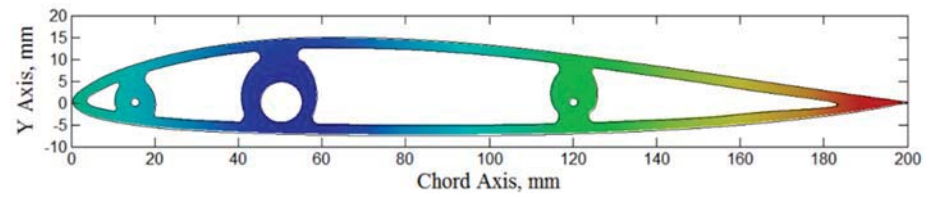
(a)



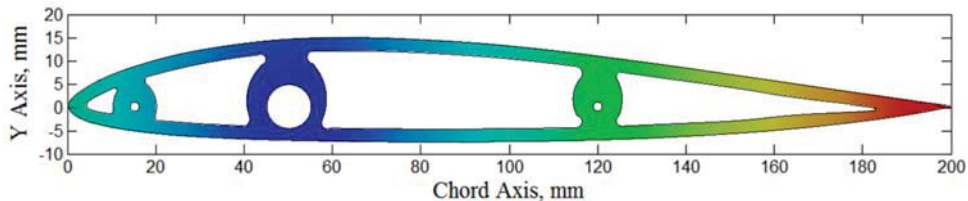
(b)



(c)



(d)



(e)

Fig. 9 Rib deformation under aerodynamic load (wash-out): (a) $t=1\text{mm}$, (b) $t=1.5\text{mm}$, (c) $t=2\text{mm}$, (d) $t=2.5\text{mm}$, and (e) $t=3\text{mm}$

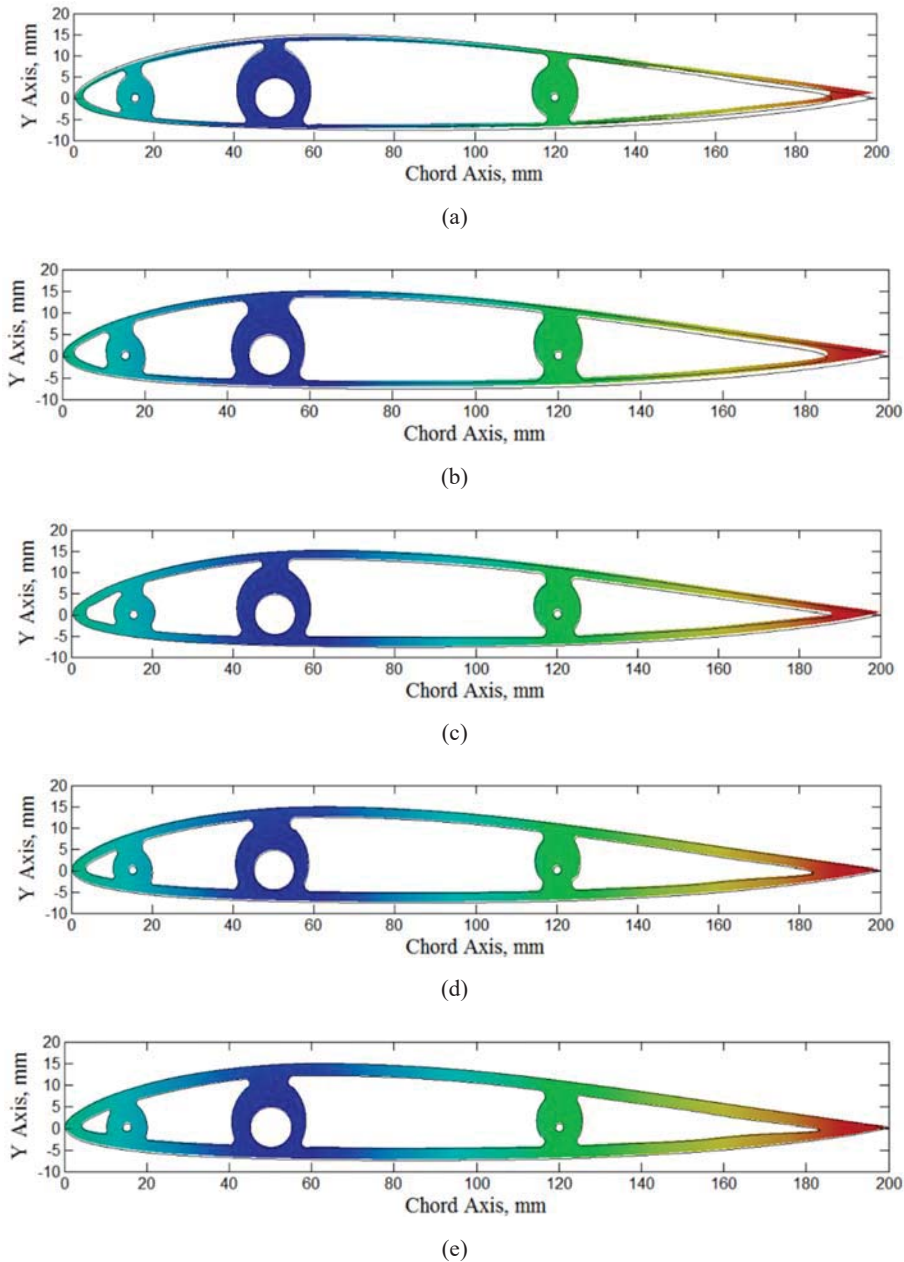


Fig. 10 Rib deformation under aerodynamic load (wash-in): (a) $t=1\text{mm}$, (b) $t=1.5\text{mm}$, (c) $t=2\text{mm}$, (d) $t=2.5\text{mm}$, and (e) $t=3\text{mm}$

Furthermore, it can be clearly seen that ribs (wing skin and/or surface) show a maximum stress of 2.5MPa (Fig. 6 (b)), much less than the material yield stress (laser ply wood) as is shown in Table I.

Contour plots (Figs. 7 and 8) illustrate the wash-out and wash-in effects of 5 different rib configurations. For clarity, undeformed geometries are also shown. Morphing twist angle was determined by measuring relative displacement of the trailing edge of the wing-tip. Overall, total displacement for both wash-in and wash-out cases increased with reduced rib edge thicknesses (t). This would be expected (again with reducing overall structural weight). Shown in Fig. 7 (e), the displacement is greater (21.76mm) for $t=1\text{mm}$ compared to 18.4mm in Fig. 8 (e). A proportion of these differences may also reflect

differences between negative and positive twist cases; aerodynamic loading tends to assist twist in the former and retard twist in the latter.

Although, small edge thickness ($t=1\text{mm}$) provides the highest twist deflections another priority is to achieve minimum surface wrinkling; i.e. a low drag profile. Figs. 9 and 10 depict the maximum surface deformation on the difference configurations. It can be seen that the minimum surface deformation exists for $t=3\text{mm}$ (as shown in Figs. 9 (e) and 10 (e)). One reason for this result lies in the reduced capability for twist of the wing's structure. As is shown in Fig. 9 (d), analysis also suggests almost no deformation (maximum of 0.49mm) of any one rib. Similar results were also obtained for $t=2\text{mm}$. According to the results, Figs. 9 (c) and 10 (c), poses reasonable

surface deformation, at 0.524mm which is still considered acceptable for the application considered. Comparing these cases with Fig. 10 (b), ($t=1.5\text{mm}$), a 1.07mm maximum bending deflection of the rib structure occurred lies outside minimum conditions specified (maximum 0.59mm). An edge thickness of $t=2\text{mm}$ therefore is considered the optimal case. Further reduction of rib edge thickness to 1mm resulted in large degrees of wing twist deflection, but excessive deformation (maximum 1.16 mm) as shown in Fig. 10 (e).

V. CONCLUSION

A numerical analysis for a novel morphing wing-twist concept is investigated structurally. In general, analysis using FEM showed that all configurations tested resulted in acceptable stress levels. Comparisons indicated a rib edge thickness of $t=2\text{mm}$ enables the preservation of adequate surface continuity with sufficient wing twist capability. The viability of this concept as for morphing applications thus seems plausible giving its ability to provide sufficient structural compliance in twist, adequate bending resistance, which maintaining an aerodynamically smooth surface finish.

REFERENCES

- [1] Culick, F. (2003). The Wright Brothers: First Aeronautical Engineers and Test Pilots. *AIAA Journal*, 41(6), 985–1006.
- [2] McRuer, D. & Graham, D. (2004). Flight control century: triumphs of the systems approach. *Journal of Guidance, Control, and Dynamics*, 27(2), 161–173.
- [3] Jha K. & Kudva J. N. (2004). Morphing aircraft concepts, classifications, and challenges. *Industrial and Commercial Applications of Smart Structures Technologies*, 5388, 213–224.
- [4] Barbarino, S. et al. (2011). A Review of Morphing Aircraft, *Journal Intelligent Materials, Systems and Structures*, 22(9), 823–877.
- [5] Kaygan, E., Gatto, A. (2014), 'Investigation of Adaptable Winglets for Improved UAV Control and Performance', *International Science Index 91, International Journal of Mechanical, Aerospace, Industrial and Mechatronics Engineering*, 8(7), 1289 - 1294.
- [6] Kaygan, E. Gatto, A. (2015), 'Computational Analysis of Adaptable Winglets for Improved Morphing Aircraft Performance', *International Science Index 103, International Journal of Mechanical, Aerospace, Industrial, Mechatronic and Manufacturing Engineering*, 9(7), 1069-1075.
- [7] Kaygan, E., Gatto, A. (2016), 'Development of an Active Morphing Wing with Novel Adaptive Skin for Aircraft Control and Performance', *The Greener Aviation 2016*, Brussels, Belgium.
- [8] G. Murray, F. Gandhi, and C. Bakis, "Flexible Matrix Composite Skins for One-dimensional Wing Morphing," *J. Intell. Mater. Syst. Struct.*, vol. 21, no. 17, pp. 1771–1781, 2010.
- [9] K. R. Olympio, F. Gandhi, L. Asheghian, and J. Kudva, "Design of a Flexible Skin for a Shear Morphing Wing," *J. Intell. Mater. Syst. Struct.*, vol. 21, no. 17, pp. 1755–1770, 2010.
- [10] E. a. Bubert, B. K. S. Woods, K. Lee, C. S. Kothera, and N. M. Wereley, "Design and Fabrication of a Passive 1D Morphing Aircraft Skin," *J. Intell. Mater. Syst. Struct.*, vol. 21, no. 17, pp. 1699–1717, 2010.
- [11] I. Dayyani, S. Ziaei-Rad, and M. I. Friswell, "The mechanical behavior of composite corrugated core coated with elastomer for morphing skins," *J. Compos. Mater.*, vol. 48, no. 13, pp. 1623–1636, 2013.
- [12] A. D. Shaw, I. Dayyani, and M. I. Friswell, "Optimisation of composite corrugated skins for buckling in morphing aircraft," *Compos. Struct.*, vol. 119, pp. 227–237, Jan. 2015.
- [13] Saffman, P. (1992). *Vortex Dynamics*, Cambridge Univ. Press, Cambridge, 46–48.
- [14] Barlow, J. B., Rae, W. H., Jr., and Pope, A., *Low-Speed Wind Tunnel Testing*, 3rd ed., Wiley-Interscience, New York, 1999.